Peter Brößner*†, Benjamin Hohlmann†, Kristian Welle, Klaus Radermacher

Validation of Automated Ultrasound-based Registration for Navigated Scaphoid Fixation

Evaluation of registration performance regarding simulated screw placement

Abstract: Fractures of the scaphoid bone may be treated in a minimally-invasive fashion. Conventionally, fluoroscopy is required to guide the placement of an osteosynthesis screw. In this work, an alternative method based on volumetric ultrasound is validated.

Methods: The fully automatic and fast image processing pipeline involves two machine learning architectures for segmentation and registration. A pre-operatively acquired 3D bone model is registered to the 3D bone surface segmented from the intra-operative ultrasound. Screw positioning is planned in an automated fashion and evaluated in an in-vitro setting: Volumetric ultrasound images of a 3D-printed phantom of a human wrist are acquired for 22 different probe poses. For 220 test runs with different initial displacements, the resulting screw placement within a defined safe zone is evaluated. If the screw lies within the safe zone, its placement is assumed to be successful.

Results: An isolated analysis of the registration results in a surface distance error of the registered meshes of 0.49 ± 0.01mm, with successful screw placement in all of the evaluated 220 test runs. The full pipeline, combining segmentation and registration, achieves a mean surface distance error of 0.79 ± 0.37mm, leading to successful screw placements for 149 out of 220 test runs. Poses not suited for the registration could be determined. Excluding these from the analysis, 139 out of 160 test runs are successful.

Conclusion: The method proves to be promising when evaluating the registration alone, even given the challenging setup of sub-optimal probe positions. The experiments also demonstrate that further improvement regarding the segmentation is necessary.

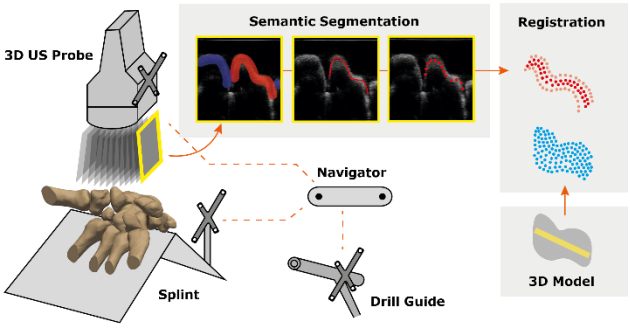

Figure 1: Proposed intraoperative procedure for the automated registration of a preoperative surgical plan based on ultrasound imaging.

Keywords: Ultrasound imaging, machine learning, segmentation, registration, scaphoid fixation

https://doi.org/10.1515/cdbme-2021-1025

1 Introduction

Fractures of the scaphoid make up for 70% of all carpal bone fractures [1]. Patients may be treated conservatively with a cast. In severe cases with dislocation or loss of blood supply, operative treatment is indicated. Furthermore, it facilitates faster recovery. Surgery can be executed in an open or minimally-invasive setting, with the latter decreasing blood loss. During surgery, the bone fragments are united using an osteosynthesis screw, which is placed under continuous fluoroscopy. This exposes the patient and especially the surgeon to substantial radiation [2].

As the diagnosis is based on a comprehensive pre-operative imaging, including computed tomography, navigated surgery is an option. Several cadaveric studies on navigated placement show that x-ray exposure time for the surgeon can be significantly reduced while maintaining the accurate positioning of the screw [3–5]. Liu et al. even propose a robotic approach and proof its feasibility in a clinical study, eliminating radiation exposure for the surgeon [6].

Beek et al. investigated ultrasound as an alternative intra-operative imaging technology, sparing both, the surgeon and

†**Both authors contributed equally**
***Corresponding author: Peter Brößner:** Chair of Medical Engineering, RWTH Aachen University, Aachen, Germany, e-mail: broessner@hia.rwth-aachen.de
Benjamin Hohlmann, Klaus Radermacher: Chair of Medical Engineering, RWTH Aachen University, Aachen, Germany
Kristian Welle: Orthopedics and Traumatology, University Clinic Bonn, Germany

patient from ionizing radiation [7]. Their approach requires the acquisition of several images and a manual registration of the pre-operative plan. While increasing the operation time, their technique allows for exact screw placement. Anas et al. further improved on the accuracy and surgery time using statistical shape models and validated the approach in an ex-vivo study. However, their registration technique still requires manual interaction and takes up to 20 minutes [8]. In a previous publication, our group proposed a deep learning based approach, reducing the processing time to seconds while eliminating the need for manual interaction [9]. In this work, we further investigate the accuracy of screw placement using a safe-zone based evaluation.

2 Methods

2.1 Automated Screw Planning

The screw position for scaphoid fixation is automatically planned by maximizing the screw length inside a safe zone, as proposed by Leventhal et al. [10]. This safe zone is derived as an inner isosurface to the surface of the bone model, at the summed distance of the screw radius (1.5mm) and an estimated cortical thickness of 0.35mm. An automatically planned screw axis can be seen in Figure 3. For a volar approach, this planning method is reported to avoid obstruction of the insertion point by the trapezium and to allow screw placement in the central third. As a safety margin, we reduced the estimated screw length by 1mm on each end.

2.2 Registration Pipeline

The bone model including the planned axis is registered to US images of a scaphoid phantom by the two stage approach depicted in Figure 1: First, a Deeplabv3+ [11] with MobileNetv2 backbone is employed for the 2D segmentation of acquired slice images. The segmented scaphoid pixels of all slices are then thinned utilizing a skeletonization algorithm and transformed to a point set. After removing statistical outliers, 1024 points are uniformly sampled from the remaining points. Finally, PRNet [12] is used to register the model point set to this sampled point set, followed by an iterative closest point (ICP) algorithm for local convergence.

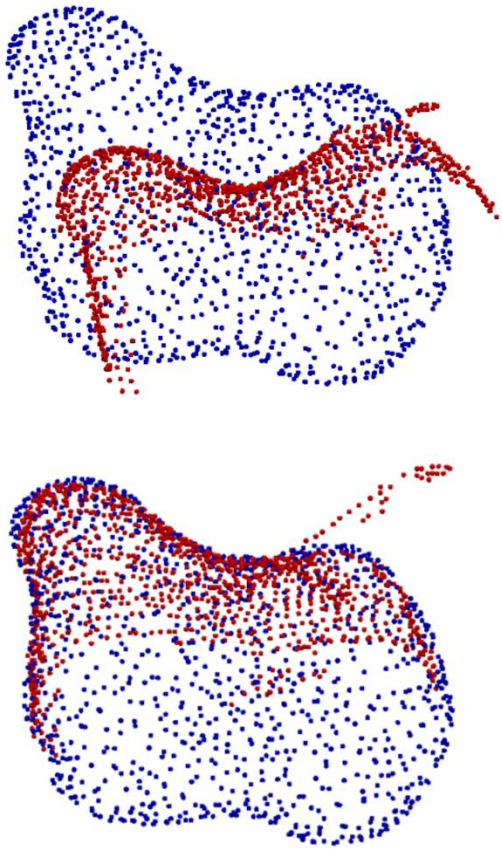

Figure 2: Example of registration for setup “P”, with initial point sets (upper image) and registered point sets (lower image).

2.3 Setup for Evaluation

Two setups are evaluated: In the first setup “GT”, the segmentation ground truth (GT) annotation is utilized as a starting point for the previously described extraction of surface points. This excludes segmentation errors and thus allows for an isolated evaluation of the registration. In the second setup “P”, the full pipeline is applied, where surface points are extracted from the segmentation predicted by the Deeplabv3+ architecture. This setup includes segmentation errors and represents the proposed workflow in surgical routine.

For the assessment of registration errors in the two setups, 10 different displacements are simulated by applying random initial transformations to the extracted surface points, with rotation sampled from uniformly distributed Euler angles in [0°, 45°] and an average translation of 3.5mm determined by demeaning. After registration, the registration error is derived by comparing initial transformation to estimated transformation.

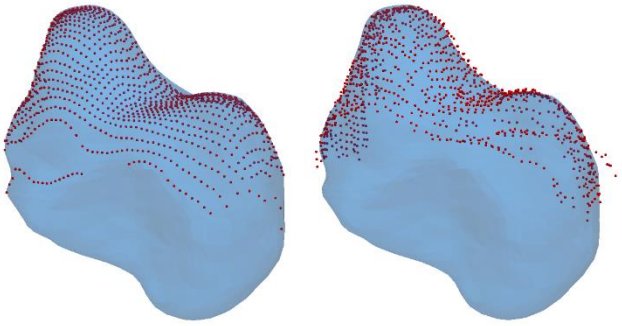

Figure 3: Points extracted from annotation in setup "GT" (left) compared to points extracted from predicted segmentation in setup "P" (right).

2.4 Evaluation of Screw Placement

The screw placements are evaluated on US images acquired from one scaphoid phantom at 22 probe poses: 5 poses rotated about the transversal axis, with the 3rd pose being centered above the scaphoid, 4 poses rotated about the longitudinal axis, starting at the proximal end and ending at the tubercle and 2 poses centered above the scaphoid, but rotated about the imaging direction. Images were captured for these 11 poses from two different distances. For each of the resulting 22 probe poses, registration is evaluated on 10 runs.

For the evaluation of screw placement, the theoretical deviation from the planned screw axis due to registration error is considered. For this purpose, the screw axis was rotated and translated according to the respective rotational and translational errors. For all transformed screw axes remaining within the safe zone, a penetration of the cortical bone is avoided and thus the placement was considered successful. For all screw axes intersecting the safe zone, screw placement was considered failed (see Figure 3).

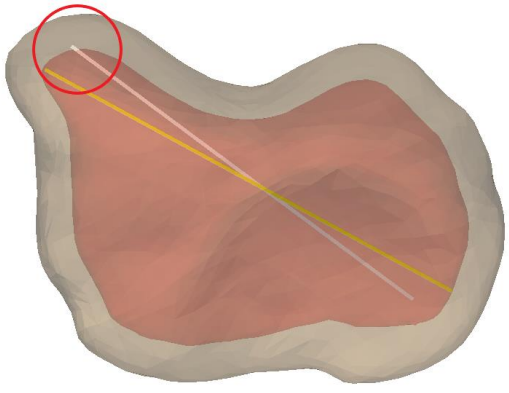

Figure 4: Example of planned screw axis (yellow) and deviation caused by registration error (white). Placement is invalid due to an intersection of the safe zone (red).

3 Results

We achieved a mean surface distance error (SDE) of 0.79 ± 0.37mm for registration on segmentation predictions (setup "P"), with a rotational error of 10.20 ± 11.32° and a translational RMSE of 0.70 ± 1.02mm. A successful screw placement was achieved for 149 out of 220 cases. A detailed breakdown for all poses can be seen in Table 1. For registration in setup "GT", a significantly lower mean SDE of 0.49 ± 0.01mm was found, with a rotational error of 1.63 ± 1.20° and a translational RMSE of 0.18 ± 0.04mm. A successful screw placement was achieved in all 220 cases. The distribution of rotational and translational errors for the 220 test runs is shown in Figure 4.

Table 1: Rotational and translational registration errors as well as valid screw placements for each probe pose in setup "P".

Probe Pose	Registration Errors	Valid Screws
Pose 1	6.72°±4.99°, 0.17mm±0.05mm	8/10
Pose 2	7.71°±4.61°, 0.20mm±0.01mm	5/10
Pose 3	1.67°±1.11°, 0.15mm±0.04mm	10/10
Pose 4	6.47°±4.65°, 0.21mm±0.08mm	9/10
Pose 5	11.78°±5.33°, 0.40mm±0.29mm	4/10
Pose 6	23.65°±9.70°, 2.45mm±0.23mm	0/10
Pose 7	15.61°±6.11°, 0.34mm±0.34mm	2/10
Pose 8	2.59°±1.49°, 0.18mm±0.03mm	10/10
Pose 9	2.94°±1.48°, 0.17mm±0.03mm	10/10
Pose 10	3.65°±1.01°, 0.22mm±0.04mm	10/10
Pose 11	5.64°±0.52°, 0.30mm±0.05mm	9/10
Pose 12	2.11°±0.43°, 0.16mm±0.04mm	10/10
Pose 13	3.96°±1.84°, 0.11mm±0.06mm	10/10
Pose 14	2.73°±1.18°, 0.32mm±0.10mm	10/10
Pose 15	4.27°±0.95°, 0.18mm±0.04mm	10/10
Pose 16	22.55°±13.68°, 1.53mm±1.32mm	2/10
Pose 17	33.44°±9.76°, 2.85mm±0.37mm	2/10
Pose 18	28.61°±3.90°, 2.01mm±0.29mm	0/10
Pose 19	2.15°±0.83°, 0.14mm±0.03mm	10/10
Pose 20	5.16°±2.69°, 0.04mm±0.27mm	8/10
Pose 21	3.04°±0.48°, 0.10mm±0.02mm	10/10
Pose 22	27.88°±10.11°, 3.05mm±0.87mm	0/10

4 Discussion

In [8], Anas et al. reported results on 13 cadaver wrists, for a rather optimal probe placement. They achieved a mean SDE

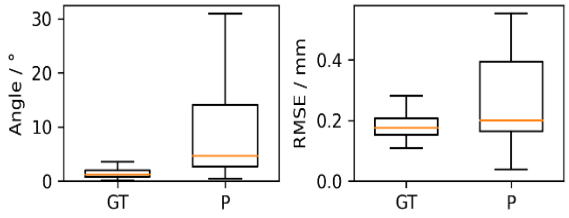

Figure 5: Boxplots of rotational (left) and translational (right) registration errors for the two setups respectively.

of 0.8 ± 0.2 mm, with a successful screw placement in 10 of 13 cases. In comparison, our approach showed a lower ratio of successful screw placements, with a comparable SDE of 0.79 ± 0.37mm (setup "P"). Based on segmentation annotations (setup "GT"), we achieved a higher percentage of successful screw placements with a lower SDE of 0.49 ± 0.01mm. However, we evaluated our approach in-vitro using only one printed wrist phantom, with images acquired from 22 different poses. These prerequisites and our focus on the evaluation of robustness to poor probe placement leads to a rather limited comparability with the results reported by Anas et al.

A significant difference can be seen between results on segmentation annotations (setup "GT") and predictions (setup "P"): On the one hand, very good results on segmentation annotations demonstrate the general suitability of our combined approach. On the other hand, improvable results on segmentation prediction, compared to results on annotations indicate at segmentation as preliminary limitation of our combined approach.

Failed screw placement is especially found for suboptimal probe poses. In particular, an all-or-nothing behavior can be observed, where screw placement is either successful or fails completely. Certain poses exhibit this poor performance, namely 5-7 and 16-18, as well as pose 22. Pose 5 and 16 are characterized by a large rotation about the longitudinal axis of the scaphoid. Pose 6, 7, 17 and 18 depict its proximal part. The registration in these cases fails, as the tubercle is not visible, which is the most distinctive part of the scaphoids shape. This constitutes an important finding for the operating surgeon, who should avoid these poses. Excluding them from the analysis, the success rate rises to 139 out of 160 or 87%.

5 Conclusion and Outlook

For the evaluation of our combined approach to navigated scaphoid fixation, a virtual screw placement was performed in an in-vitro setup. In conclusion, we have shown the general suitability of our approach, with a complete automation and fast computation times. An analysis of the probe positions revealed poses the surgeon needs to avoid. Segmentation may need further improvement with regard to robustness to suboptimal probe placement. This may be achieved by utilizing a 3D segmentation approach for an improved exploitation of the image context. Furthermore, ex-vivo and in-vivo studies are objectives of our ongoing work.

Author Statement

Research funding: The author state no funding involved. Conflict of interest: Authors state no conflict of interest. Ethical approval: The conducted research is not related to either human or animals.

References

[1] Langer MF, Oeckenpöhler S, and Breiter S, et al., 2016,"Anatomie und Biomechanik des Kahnbeins," Orthopäde, 45(11), pp. 926–937.

[2] Singer G, 2005,"Radiation exposure to the hands from mini C-arm fluoroscopy," The Journal of Hand Surgery, 30(4), pp. 795–797.

[3] Citak M, O'Loughlin PF, and Kendoff D, et al., 2010,"Navigated scaphoid screw placement using customized scaphoid splint: an anatomical study," Arch Orthop Trauma Surg, 130(7), pp. 889–895.

[4] Kam CC, and Greenberg JA, 2014,"Computer-assisted navigation for dorsal percutaneous scaphoid screw placement: a cadaveric study," The Journal of Hand Surgery, 39(4), pp. 613–620.

[5] Walsh E, Crisco JJ, and Wolfe SW, 2009,"Computer-assisted navigation of volar percutaneous scaphoid placement," The Journal of Hand Surgery, 34(9), pp. 1722–1728.

[6] Liu B, Wu F, and Chen S, et al., 2019,"Robot-assisted percutaneous scaphoid fracture fixation: a report of ten patients," The Journal of hand surgery, European volume, 44(7), pp. 685–691.

[7] Beek M, Abolmaesumi P, and Luenam S, et al., 2008,"Validation of a new surgical procedure for percutaneous scaphoid fixation using intra-operative ultrasound," Medical Image Analysis, 12(2), pp. 152–162.

[8] Anas EMA, Seitel A, and Rasoulian A, et al., 2016,"Registration of a statistical model to intraoperative ultrasound for scaphoid screw fixation," Int J CARS, 11(6), pp. 957–965.

[9] Broessner P, Hohlmann B, and Radermacher K, 2021,"Ultrasound-based Navigation of Scaphoid Fracture Surgery," Bildverarbeitung für die Medizin 2021, 1st ed., Springer Fachmedien Wiesbaden; Imprint: Springer Vieweg, Wiesbaden, pp. 28–33.

[10] Leventhal EL, Wolfe SW, and Walsh EF, et al., 2009,"A computational approach to the "optimal" screw axis location

and orientation in the scaphoid bone," The Journal of Hand Surgery, 34(4), pp. 677–684.

[11] Chen L-C, Zhu Y, and Papandreou G, et al., 2018, Encoder-Decoder with Atrous Separable Convolution for Semantic Image Segmentation, Computer Vision - ECCV 2018: 15th European Conference, Munich, Germany, September 8-14, 2018, Proceedings, Part VII, Ferrari V., Hebert M., Sminchisescu C., and Weiss Y., eds., Springer International Publishing, Cham, pp. 833–851.

[12] Wang Y, and Solomon JM, 2019,"PRNet: Self-Supervised Learning for Partial-to-Partial Registration," Advances in Neural Information Processing Systems, Curran Associates, Inc.